Frontier Developments in Continuum Mechanics and Nonlinear Dynamics: Theories, Methods, and Applications

Habilitation thesis

Assoc. Prof. Dr. Olivia Ana Florea

Faculty of Mathematics and Computer Science
Transilvania University of Brașov, Romania

November 22, 2024

Educational Foundation

Academic Background

- Bachelor's Degree in Mathematics (1997-2001): Faculty of Mathematics and Computer Science, Transilvania University of Braşov.
- Advanced Studies Diploma in Mathematical Models and Software Products (2001-2002)
- PhD in Mechanical Engineering (2004-2010):Analytical and Numerical Methods in Solving Dynamic System Problems Applied in the Simulation of Hydraulic System Components
- Postdoctoral fellowship (2014-2015): Modeling and Simulation of Biomechanical Systems to Improve Operational Performance
- Second PhD in Mathematics (2015 -2019): Mixed Problems with Boundary and Initial Data for Generalized Continuous Media

Contributions to Teaching and Research

Teaching and Student Engagement

- I teach courses of Applied Mathematics, Theoretical Mechanics, Mathematical Analysis, Optimal Control, Multi-physics Simulations, Dynamic simulation of vehicle systems in Matlab
- Mentorship: I am passionate about guiding students through complex interdisciplinary research projects, helping them connect theoretical insights with practical applications. Now I coordinate two master thesis:
  - Optimization and Optimal Control in Automotive Systems
  - Laplace transform method for solving problems in engineering domains

Research and Impact

26 papers in WoS, 36 papers in DBI and Conferences

Continuum mechanics and fluid mechanics:
Continuum Mechanics And Thermodynamics (**2024, 2021**),
Waste And Biomass Valorization (**2022**),
Mathematics And Mechanics Of Solids (**2019**),
Symmetry (**2019**)
International Journal Of Applied Mechanics (**2017**)
Boundary Value Problems (**2015**)
Mathematical Problems In Engineering (**2015**)

Dynamical systems:
Physics Letters A (**2023**),
Scientific Annals of Ovidius University of Constanta (**2023, 2020, 2015, 2014**)
Acta Technica Napocensis Series-Applied Mathematics Mechanics And Engineering (**2020, 2015**),
Plos One (**2015**)
Aip Advances (**2016**)
Canadian Journal Of Physics (**2015**)

MINIMAL STANDARDS FOR HABILITATION THESIS

SRECENT =Sum(SRI Journal/number of authors) from the last 7 years =**5.008175** >=2.5
S = Sum(SRI Journal/number of authors)=**6.958342**>=5
117 Times Cited Total.
99 Times Cited Without self-citations.
43 Citations in journals with SRI>=**0.5**

Objective: Purpose and Scope of the Thesis

Purpose of the Thesis

- The present thesis aims to contribute to the fields of continuum mechanics and nonlinear dynamics, particularly through theoretical advancements, innovative numerical methods, and practical applications.
- The thesis bridges theoretical research with real-world applications, showing how rigorous mathematical frameworks and numerical methods can solve complex material science problems.

Main Topics Covered

My reseach spans three main topics:

- Advanced theoretical insights in the **thermoelasticity of double porous materials**.
- Advanced **numerical methods for nonlinear dynamical systems**.
- Innovative **modeling approaches in nanomaterials and biomass analysis**.

Chapter 1. Advanced Theoretical Insights in Thermoelasticity of Double Porous Materials

- The first chapter focuses on my research in continuum mechanics, specifically on thermoelastic materials with double porosity structures
- This chapter is an extension of my PhD thesis in Mathematics, completed in 2019, and presents significant advancements in understanding the complex interactions between thermal and mechanical behaviors in materials with double porosity.

1.1. Some uniqueness results for thermoelastic materials with double porosity structure

Emin, A. N., Florea, O.A., Craciun, E.M., Continuum Mech. Thermodyn, 33: 1083–1106, 2021.

- **Concept**: Double porous materials contain two interconnected pore structures, which can include both microscopic voids and macroscopic cracks. These materials exhibit complex mechanical and thermal responses due to their unique structure.
- **Applications**: Relevant in civil engineering (soil mechanics, geotechnics) and biomechanics (e.g., porous bone structures).
- **Historical Context:** The study of materials with double porosity starts with models by Barenblatt and has expanded to incorporate thermoelasticity, taking into both thermal and mechanical interactions.

The equations that model material with two porosities are:

$$\begin{aligned} \rho\ddot{u}_i &= t_{ji,j} + \rho F_i, \\ \kappa_1\ddot{\varphi} &= \sigma_{j,j} + p + \rho M, \\ \kappa_2\ddot{\psi} &= \tau_{j,j} + r + \rho N, \end{aligned} \tag{1}$$

It contains: the displacement equations that take into account the direct forces that act on the body; the stress tensors and the volume fraction equations for the porosities.
ρ = the density of material; u_i =the displacement
κ_1, κ_2 = the equilibrated inertia coefficients
φ, ψ = the volume fraction fields
σ_j, τ_j= the vectors of the equilibrated stress
t_{ij} = the stress tensors at the body's surface ∂B.
p, r = the intrinsic forces, F_i = the direct forces, M = the extrinsic forces that act on the pores, N = the extrinsic forces that act on the cracks.

The energy's equation for the thermoelastic double porous material:

$$\rho T_0 \dot{\eta} = q_{j,j} + \varrho\delta, \tag{2}$$

It relates entropy rate changes to heat flux and heat supply over time.
T_0 = absolute temperature from the reference configuration
η = the entropy; q_j= the heat flux; δ = the heat supply
Using this equation alongside the motion equations (1), we derive the compresive model shown in (3):

$$\begin{aligned}
&\rho\ddot{u}_i = \left(C_{jikl}u_{k,l} + B_{ji}\varphi + D_{ji}\psi - \beta_{ji}\theta\right)_{,j} + \rho F_i,\\
&\kappa_1\ddot{\varphi} = \left(\alpha_{ij}\varphi_{,i} + b_{ij}\psi_{,i}\right)_{,j} - B_{ij}u_{i,j} - \alpha_1\varphi - \alpha_3\psi + \gamma_1\theta + \rho M,\\
&\kappa_2\ddot{\psi} = \left(b_{ij}\varphi_{,i} + \gamma_{ij}\psi_{,i}\right)_{,j} - D_{ij}u_{i,j} - \alpha_3\varphi - \alpha_2\psi + \gamma_2\theta + \rho N,\\
&aT_0\dot{\theta} = -T_0(\beta_{ij}\dot{u}_{i,j} + \gamma_1\dot{\varphi} + \gamma_2\dot{\psi}) + (K_{ij}\theta_{,j})_{,j} + \rho\delta.
\end{aligned} \tag{3}$$

The initial and boundary conditions for the mixed problem are provided in (4) & (5). These conditions specify the behaviour of displacements, volume fractions, entropy and temperature at the initial time and on the boundaries, respectively.

The initial conditions are:

$$\begin{array}{l} u_i(x_0,0) = u_i^0(x_0),\ \dot{u}_i(x_0,0) = v_i^0(x_0), \\ \varphi(x_0,0) = \varphi_0(x_0),\ \dot{\varphi}(x_0,0) = \tilde{\varphi}_0(x_0),\ x_0 \in \bar{B}. \\ \psi(x_0,0) = \psi_0(x_0),\ \dot{\psi}(x_0,0) = \tilde{\psi}_0(x_0) \\ \eta(x_0,0) = \eta_0(x_0), \end{array} , \tag{4}$$

The boundary conditions are:

$$\begin{array}{llllll} u_i = u_i^b & \text{on} & \partial B_1 \times [0,\infty), & t_i = t_i^b & \text{on} & \partial B_1^c \times [0,\infty), \\ \varphi = \varphi^b & \text{on} & \partial B_2 \times [0,\infty), & \lambda = \lambda^b & \text{on} & \partial B_2^c \times [0,\infty), \\ \psi = \psi^b & \text{on} & \partial B_3 \times [0,\infty), & m = \omega^b & \text{on} & \partial B_3^c \times [0,\infty), \\ \theta = \theta^b & \text{on} & \partial B_4 \times [0,\infty), & \nu = \Omega^b & \text{on} & \partial B_4^c \times [0,\infty), \end{array} \tag{5}$$

The ordered array $(u_i, \varphi, \psi, \theta)$ is a solution for the mixed boundary value problem of a thermoelastic material with double porosity in the cylinder $\Omega_0 = B \times [0, \infty)$.

We consider the following assumptions to ensure the well - posedness of the problem, leading to a unique and stable solution.

1. Continuity of coefficients: the constitutive coefficients, the density ρ, the coefficients of inertia κ_1, κ_2 must be continuous on $\bar{B}$;
2. Smoth external functions: the body forces F_i, the extrinsic forces M, N and the heat supply h must be continuous on the cylinder $\Omega_0 = B \times [0, \infty)$;
3. Boundary conditions: $u_i^b, \varphi^b, \psi^b, \theta^b$ must be continuous in their domains
4. External data: t_i^b, λ^b, ω^b, Ω^b are functions that are continuous in time and piecewise regular in their domains of definition.

The Betti reciprocity theorem is a fundamental result in the analysis of the thermoelastic double porous materials.
It establishes a relation between two systems of external loads $H^{(1)}, H^{(2)}$ and the solutions corresponding to these loads $S^{(1)}, S^{(2)}$.

The external loads include: body forces, heat supply, extrinsic forces, prescribed initial conditions:

$$\begin{aligned} H^{(a)} = \{ & F_i^{(a)}, \omega^{(a)}, M^{(a)}, \delta^{(a)}, u_i^{*(a)}, t_i^{*(a)}, \varphi^{*(a)}, \lambda^{*(a)}, \psi^{*(a)}, \\ & \omega^{*(a)}, \theta^{*(a)}, \Omega^{*(a)}, u_i^{0(a)}, v_i^{0(a)}, \varphi_0^{(a)}, \tilde{\varphi}_0^{(a)}, \psi_0^{(a)}, \tilde{\psi}_0^{(a)}, \eta_0^{(a)} \}, \end{aligned} \tag{6}$$

The solutions consist of: displacements, volume fraction fields, stress tensors, heat fluxes.

$$S^{(a)} = \{ u_i^{(a)}, \varphi^{(a)}, \psi^{(a)}, \theta^{(a)}, t_{ij}^{(a)}, \sigma_i^{(a)}, \tau_i^{(a)}, q_i^{(a)}, r^{(a)}, p^{(a)} \}, \tag{7}$$

where: $t_i^{(a)} = t_{ij}^{(a)} n_j, \quad \lambda^{(a)} = \sigma_i^{(a)} n_i, \quad \omega^{(a)} = \tau_i^{(a)} n_i, \quad \Omega^{(a)} = q_i^{(a)} n_i.$

The uniqueness theorem which ensures that the mixed problem for the thermoelastic double porous materials has unique solution

Theorem

If the assumptions above are fulfilled then the mixed problem for thermoelastic bodies with double porosity (3) *accompanied by the initial conditions* (4) *and the boundary conditions* (5) *admits a unique solution.*

This theorem is fundamental for modeling thermoelastic materials in engineering, ensuring reliable predictions of material behavior under varying thermal and mechanical loads.

Next reciprocity theorem is a result derived from Betti reciprocity relation.

Theorem

For two systems of external loads $H^{(1)}, H^{(2)}$ with corresponding solutions $S^{(1)}, S^{(2)}$, the following integral relation holds:

$$\begin{aligned}
&\int_B [F_i^{(1)} * u_i^{(2)} + \omega^{(1)} * \varphi^{(2)} + N^{(1)} * \psi^{(2)} - \tfrac{1}{\rho T_0}\xi * \omega^{(1)} * \theta^{(2)}]\, dV \\
&+ \int_{\partial B} [\xi * (t_i^{(1)} * u_i^{(2)} + \lambda^{(1)} * \varphi^{(2)} + \omega^{(1)} * \psi^{(2)} - \tfrac{1}{\rho T_0}\Omega^{(1)} * \theta^{(2)})]\, dA \\
&= \int_B [F_i^{(2)} * u_i^{(1)} + \omega^{(2)} * \varphi^{(1)} + N^{(2)} * \psi^{(1)} - \tfrac{1}{\rho T_0}\xi * \omega^{(2)} * \theta^{(1)}]\, dV \\
&+ \int_{\partial B} [\xi * (t_i^{(2)} * u_i^{(1)} + \lambda^{(2)} * \varphi^{(1)} + \omega^{(2)} * \psi^{(1)} - \tfrac{1}{\rho T_0}\Omega^{(2)} * \theta^{(1)})]\, dA,
\end{aligned} \tag{8}$$

This theorem is essential for:
- Validating the physical consistency of models
- Analyzing the effects of different load scenarios
- Ensuring the robustness of materials under varying operational conditions in applications like civil engineering and material science

The following lemma provides an important result for establishing uniqueness in thermoelastic media with double porosity.

Lemma

Based on the above, the following differential relationship occurs:

$$
\begin{aligned}
&\frac{d}{d\zeta}\Big[\int_B (\rho u_i(\xi)u_i(\xi) + \kappa_1\varphi(\xi)\varphi(\xi) + \kappa_2\psi(\xi)\psi(\xi))\, dV + \frac{1}{\rho T_0}\int_0^\xi \int_B K_{ij}\theta_{*,i}(\xi)\theta_{*,j}(\xi)\, dV\, d\zeta\Big] \\
&- \int_B [\rho(u_i(2\xi)\dot{u}_i(0) + \dot{u}_i(2\xi)u_i(0)) + \kappa_1(\varphi(2\xi)\dot{\varphi}(0) + \dot{\varphi}(2\xi)\varphi(0)) + \kappa_2(\psi(2\xi)\dot{\psi}(0) + \dot{\psi}(2\xi)\psi(0))]\, dV = \\
&= \int_0^\xi \int_B [\rho F_i(\xi-\zeta)u_i(\xi+\zeta) + \lambda(\xi-\zeta)\varphi(\xi+\zeta) + m(\xi-\zeta)\psi(\xi+\zeta) - \frac{1}{\rho T_0}\omega(\xi-\zeta)\theta(\xi+\zeta)]\, dV\, d\zeta \\
&- \int_0^\xi \int_B [\rho F_i(\xi+\zeta)u_i(\xi-\zeta) + \lambda(\xi+\zeta)\varphi(\xi-\zeta) + m(\xi+\zeta)\psi(\xi-\zeta) - \frac{1}{\rho T_0}\omega(\xi+\zeta)\theta(\xi-\zeta)]\, dV\, d\zeta \\
&+ \int_0^\xi \int_{\partial B} [t_i(\xi-\zeta)u_i(\xi+\zeta) + \lambda(\xi-\zeta)\varphi(\xi+\zeta) + m(\xi-\zeta)\psi(\xi+\zeta) - \frac{1}{\rho T_0}\Omega_*(\xi-\zeta)\theta(\xi+\zeta)]\, dA\, d\zeta \\
&- \int_0^\xi \int_{\partial B} [t_i(\xi+\zeta)u_i(\xi-\zeta) + \lambda(\xi+\zeta)\varphi(\xi-\zeta) + m(\xi+\zeta)\psi(\xi-\zeta) - \frac{1}{\rho T_0}\Omega_*(\xi+\zeta)\theta(\xi-\zeta)]\, dA\, d\zeta.
\end{aligned}
\tag{9}
$$

This relation demonstrates the balance of energy across the material volume B, involving mechanical displacements u_i, volume fractions ϕ, ψ, and thermal gradients θ.

Theorem

If the thermal conductivity tensor K_{ij} is positive definite and the assumptions above are satisfied, then the mixed problem, consisting of: the governing equations (3), initial conditions (4), boundary conditions (5), admits a unique solution.

This theorem guarantees that, under realistic physical assumptions, the model remains mathematically consistent and reliable for analyzing complex thermoelastic behavior in double porous materials.

Implications:

- Ensures predictability and robustness of material models in applications like geotechnics and biomechanics.
- Forms the basis for validating simulations and theoretical predictions in complex material systems.

1.2. Moore–Gibson–Thompson thermoelasticity in the context of double porous materials

Florea, O.A., Bobe, A., Continuum Mech. Thermodyn., 33:2243–2252, 2021.

- **Theory Overview:** The MGT thermoelasticity model introduces a framework that considers finite thermal wave speeds, crucial for accurately modeling heat propagation in materials exposed to rapid temperature changes.
- **Application to Double Porous Materials:** MGT theory has been adapted to model double porous structures, allowing for the simulation of interactions between thermal and mechanical fields.
- **Importance:** Essential for applications where materials undergo rapid temperature fluctuations, such as in geothermal energy systems or aerospace applications where temperature and mechanical stress must be tightly controlled to prevent failure.

The differential Moore-Gibson-Thompson (MGT) equation for thermoealsticity incorporating the Maxwell-Cattaneo law to account for finite thermal wave speeds.

$$\gamma \cdot c(x)\frac{d^3\theta}{dt^3} + c(x)\frac{d^2\theta}{dt^2} = \left(K_{ij}(x)\theta_{,i} + K^*_{ij}(x)\theta_{,i}\right)_{,j} \tag{10}$$

$\gamma=$ the thermal relaxation parameter, ensuring that heat propagation occurs at finite speeds; $c(x)=$ Specific heat capacity, varying spatially across the material domain. $\theta =$ Temperature field, representing the thermal state of the material. $K_{ij}(x)$ and $K^*_{ij}(x)=$ Tensorial coefficients for thermal conductivity, modeling directional and material-dependent heat transfer.

- The presence of higher-order time derivatives $\frac{d^3\theta}{dt^3}$ reflects advanced thermal wave modeling, enabling predictions of rapid thermal transients.
- The coupling with conductivity tensors accounts for anisotropic heat flow, relevant in materials with directional porosities.

the initial conditions in the context of MGT theory of thermoelasticity for materials with double porosity structure

$$
\begin{aligned}
&u_i(x,0)=0;\ \phi(x,0)=0;\ \psi(x,0)=0;\ \theta(x,0)=0\\
&\dot{u}_i(x,0)=0;\ \dot{\phi}(x,0)=0;\ \dot{\psi}(x,0)=0;\ \dot{\theta}(x,0)=0;\ \ddot{\theta}(x,0)=0
\end{aligned}
\tag{11}
$$

These initial conditions provide a baseline for the system, ensuring that the response is solely due to external inputs, such as applied forces or heat sources.

The mixed problem for the MGT theory has the boundary conditions:

$$
\begin{aligned}
&u_i=u_i^* \text{ on } \partial\Omega_1\times[0,t^*);\ t_i=t_i^* \text{ on } \partial\Omega_1^c\times[0,t^*)\\
&\phi=\phi^* \text{ on } \partial\Omega_2\times[0,t^*);\ \lambda=\lambda^* \text{ on } \partial\Omega_2^c\times[0,t^*)\\
&\psi=\psi^* \text{ on } \partial\Omega_3\times[0,t^*);\ m=\omega^* \text{ on } \partial\Omega_3^c\times[0,t^*)\\
&\theta=\theta^* \text{ on } \partial\Omega_4\times[0,t^*);\ \nu=\Omega^* \text{ on } \partial\Omega_4^c\times[0,t^*)
\end{aligned}
\tag{12}
$$

The energy equation will have the following form:

$$\rho T_0 \left[\beta_{ij}\dot{u}_{i,j} + a_1\dot{\phi} + a_2\dot{\psi} + c(\gamma\dddot{\theta} + \ddot{\theta})\right] = (K_{ij}\theta_{,j})_{,i} + \rho\delta \tag{13}$$

- Thermal Inertia ρT_0: the material's resistance to temperature changes.
- Mechanical Coupling $\beta_{ij}\dot{u}_{i,j}$: the influence of mechanical displacement gradients $\dot{u}_{i,j}$ on the energy balance.
- Porosity Dynamics $a_1\dot{\phi} + a_2\dot{\psi}$: the contributions from changes in the volume fractions ϕ, ψ of the two porosity fields.
- Thermal Relaxation $(\gamma\dddot{\theta} + \ddot{\theta})$: The second $\ddot{\theta}$ and first-order $\dot{\theta}$ time derivatives capture finite propagation speeds of thermal waves
- Heat Conduction $(K_{ij}\theta_{,j})_{,i}$: the flow of heat through the material
- External Heat Supply $\rho\delta$: the contribution of external heat sources to the overall energy balance.

The energy function of MGT thermoelasticity is expressed as: $\mathbb{E} = E_i - \eta\Phi$
E_i= the internal energy, capturing contributions from displacement, porosities, and thermal fields;
$\eta\Phi$= a term accounting for the dissipative effects in the system.

The energy function $\mathbb{E}$ will have the following quadratic expression:

$$\mathbb{E}=\frac{1}{2}C_{ijkl}u_{i,j}u_{k,l}+B_{ij}\phi u_{i,j}+D_{ij}\psi u_{i,j}+\frac{1}{2}\phi_{,i}\phi_{,j}+b_{ij}\phi_{,i}\psi_{,j}+\frac{1}{2}\gamma_{ij}\psi_{,i}\psi_{,j}+ \tag{14}$$
$$+\frac{1}{2}\alpha_1\phi^2+\alpha_3\phi\psi+\frac{1}{2}\alpha_2\psi^2+\frac{1}{2}K_{ij}\Theta_{,i}\theta_{,j}-A\dot{\theta}^2-B\dot{\theta}\ddot{\theta}+C\ddot{\theta}^2$$

This equation integrates all energy components, such as elastic, thermal, and coupling terms for porosities ϕ, ψ and temperature gradients θ.

The kinetic energy per mass unit is:

$$E_{\mathbb{K}}(t)=\frac{1}{2}\left[\rho\dot{u}_i(t)\dot{u}_i(t)+\kappa_1\dot{\phi}(t)\dot{\phi}(t)+\kappa_2\dot{\psi}(t)\dot{\psi}(t)\right] \tag{15}$$

These equations form the backbone of the energy analysis in thermoelastic systems, connecting displacement, porosity, and temperature dynamics under the MGT framework.

Energy Variation Theorem

The variation of energy in the MGT thermoelasticity for double porous materials is expressed by:

$$\begin{aligned}\frac{d}{dt}\int_{\Omega}(E_{\mathbb{K}}+\mathbb{E})dV=&\rho\int_{\Omega}\Big(F_i\dot{u}_i+M\dot{\phi}+N\dot{\psi}\Big)dV+\int_{\partial\Omega}\Big(t_{ji}\dot{u}_i+\sigma_j\dot{\phi}+\tau_j\dot{\psi}\Big)n_j dA+\\&+\int_{\Omega}\left(q_i\dot{\theta}_{,j}+\frac{1}{\rho T_0}(q_{i,i}+\rho\delta)(\gamma\ddot{\theta}+\dot{\theta})\right)dV-\\&-\int_{\Omega}\Big(\frac{2}{3}A(\gamma\ddot{\theta}+\dot{\theta})(\gamma\dddot{\theta}+\ddot{\theta})+(2A+B)\dot{\theta}\ddot{\theta}+B\ddot{\theta}^2+2C\ddot{\theta}\cdot\dddot{\theta}\Big)dV\end{aligned}\tag{16}$$

Stability of the System: The theorem demonstrates that if the energy function E is positive definite, the system remains stable over time, ensuring bounded and predictable behavior.

Uniqueness of the Solution: The theorem guarantees that the mixed problem has a unique solution under given initial and boundary conditions, which is essential for theoretical rigor and numerical simulations.

Real-World Applications: It validates the use of MGT thermoelasticity for advanced material designs, such as heat-resistant composites and porous structures in civil engineering and aerospace.

1.3. Green-Lindsay Thermoelasticity Theory for Double Porous Materials

Anamaria N Emin, Olivia A Florea Scientific Annals of the "Ovidius" University of Constanța. Mathematics Series 2023

- **Theory Overview:** Green-Lindsay thermoelasticity theory also extends classical thermoelastic models to accommodate finite thermal wave speeds, providing a way to predict and manage thermal responses under stress.
- **Specific Application:** By applying Green-Lindsay theory to double porous materials, this research advances understanding of how these materials react to coupled thermal and mechanical loading.
- **Engineering Relevance:** This model is instrumental in fields that deal with high thermal and mechanical stress, including civil and aerospace engineering.

Based on the Green-Lindsay theory the heat flux components are:

$$q_i = -\theta_0(b_i\dot{\theta} + K_{ij}\theta_{,j}). \tag{17}$$

q_i= Heat flux vector; θ_0=Reference temperature; b_i= Heat transfer coefficients; K_{ij}= Thermal conductivity tensor; $\dot{\theta}$= Time derivative of temperature.
This equation highlights the dependency of heat flux on both temperature gradients $\theta_{,j}$ and rate of temperature change $\dot{\theta}$.

the quadratic form of the Helmholtz energy:

$$\begin{aligned}\omega = \tfrac{1}{2}C_{ijkl}u_{k,l}u_{i,j} + B_{ij}\varphi u_{i,j} + D_{ij}\psi u_{i,j} - \beta_{ij}u_{i,j}(\theta + \alpha\dot{\theta}) + \\ + \tfrac{1}{2}a_{ij}\varphi_{,i}\varphi_{,j} + b_{ij}\varphi_{,i}\psi_{,j} + \tfrac{1}{2}\delta_{ij}\psi_{,i}\psi_{,j} + \tfrac{1}{2}\alpha_1\varphi^2 + \tfrac{1}{2}\alpha_2\psi^2 + \\ + \alpha_3\varphi\psi - \gamma_1\varphi(\theta + \alpha\dot{\theta}) - \gamma_2\psi(\theta + \alpha\dot{\theta}) + \\ + \tfrac{1}{2}c(\theta + \alpha\dot{\theta})^2 + b_i\theta_0\dot{\theta}\theta_{,i} + \tfrac{1}{2}\theta_0 K_{ij}\theta_{,i}\theta_{,j}.\end{aligned} \tag{18}$$

The equation incorporates elastic, porosity ϕ, ψ, and thermal coupling effects.

the energy equation becomes:

$$\rho\beta_{ij}\dot{u}_{i,j} + \rho\gamma_1\dot{\varphi} + \rho\gamma_2\dot{\psi} + \rho a\dot{\theta} + \rho c\alpha\ddot{\theta} + b_i\dot{\theta}_{,i} + K_{ij}\theta_{,ij} - \frac{\rho\delta}{\theta_0} = 0. \qquad (19)$$

This equation captures the equilibrium between thermal and mechanical energy contributions in the system.

The energy variation theorem for Green-Lindsay thermoelasticity in double porous materials

The energy balance for double porous materials is described as:

$$\frac{d}{dt}\int_B (\xi_c + \omega)\ dV = \rho\int_B \left(F_i\dot{u}_i + M\dot{\varphi} + N\dot{\psi} + \frac{h}{\theta_0}\left(\theta + \alpha\dot{\theta}\right)\right)\ dV + \\ + \int_{\partial B}\left(t_{ji}\dot{u}_i + \sigma_j\dot{\varphi} + \tau_j\dot{\psi}\right)n_i\ dA + \frac{1}{\rho}\int_{\partial B}\left[\frac{q_i}{\theta_0}\left(\theta + \alpha\dot{\theta}\right) + q_i\dot{\theta}\right]n_i\ dA + \int_{\partial B} b_i\theta_0\theta\ddot{\theta}n_i\ dA. \qquad (20)$$

If the energy function ω is positively defined, then the mixed problem for double porous bodies admits a unique solution.

Chapter 2. Advanced Numerical Methods in Nonlinear Dynamical Systems

- The thesis investigates complex dynamical systems through advanced numerical methods.
- By analyzing systems like the double pendulum with fractional derivatives, and the motion of a bead on a rotating wire, the thesis delves into both chaotic and periodic behaviors that traditional models often overlook.
- This work demonstrates the importance of numerical methods in capturing non-linear behaviors, which are otherwise analytically challenging, providing deeper insights for engineering and physics applications.

2.1. Fractional Features of a Double Pendulum System

Florea, D Baleanu, J Asad in *Dynamic Systems and Applications* 30 (2), 305-320, 2021

Figure 1 presents a double pendulum system, which consists of two masses m_1, m_2 connected by two lightweight rods b_1, b_2. This mechanical system demonstrates rich dynamics, including chaotic and periodic behavior, making it an ideal case study for investigating nonlinear dynamical systems.

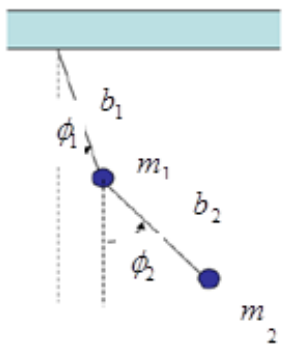

Figure 1: The double pendulum system

the kinetic and potential energies of the system:

$$T = \frac{1}{2}\left(\omega_1 + \omega_2\right) b_1^2 \dot{\varphi}_1^2 + \frac{1}{2}\omega_2 b_2^2 \dot{\varphi}_2^2 + \omega_2 b_1 b_2 \cos\left(\varphi_1 - \varphi_2\right) \dot{\varphi}_1 \dot{\varphi}_2, \quad (21)$$

This equation describes the system's kinetic energy. It combines the effects of the angular velocities of the masses and the interaction between the two pendulums.

$$V = -\left(\omega_1 + \omega_2\right) g b_1 \cos\varphi_1 - \omega_2 g b_2 \cos\varphi_2. \quad (22)$$

This represents the gravitational potential energy. It considers the relative heights of the pendulums with respect to a reference point.

the classical Lagrangian $L_c = T - V$

$$\begin{aligned} L_c \quad &= \tfrac{1}{2}\left(\omega_1 + \omega_2\right) b_1^2 \dot{\varphi}_1^2(t) + \tfrac{1}{2}\omega_2 b_2^2 \dot{\varphi}_2^2(t) + \omega_2 b_1 b_2 \cos\left(\varphi_1(t) - \right. \\ &\left. -\varphi_2(t)\right) \dot{\varphi}_1 \dot{\varphi}_2(t) + \left(\omega_1 + \omega_2\right) g b_1 \cos\varphi_1 + \omega_2 g b_2 \cos\varphi_2. \end{aligned} \quad (23)$$

Using the Lagrangian framework allows for a comprehensive analysis of the system's behavior, including chaotic dynamics under certain conditions.

The classical Lagrangian is reformulated using Caputo's fractional derivative, providing a generalized model for systems with memory effects. The fractional Lagrangian L_f is given by:

$$\begin{aligned} L_f &= \frac{(\omega_1+\omega_2)b_1^2\left({}_a^C D_t^\alpha \varphi_1(t)\right)^2+\omega_2 b_2^2\left({}_a^C D_t^\alpha \varphi_2(t)\right)^2}{2}+ \\ &+\omega_2 b_1 b_2 \cos\left(\varphi_1(t)-\varphi_2(t)\right){}_a^C D_t^\alpha \varphi_1(t){}_a^C D_t^\alpha \varphi_2(t)+ \\ &+\left(\omega_1+\omega_2\right) g b_1 \cos\varphi_1(t)+\omega_2 g b_2 \cos\varphi_2(t). \end{aligned} \tag{24}$$

$\left({}_a^C D_t^\alpha \varphi_1(t)\right)=$ Caputo fractional derivative. $\phi_1(t), \phi_2(t)=$ Angular positions of the double pendulum components. $\alpha=$ Fractional order parameter, capturing memory and hereditary effects in the system.

The fractional Hamiltonian $H_f(t)$ represents the total energy (kinetic + potential) in the fractional framework:

$$\begin{aligned} \mathrm{H}_f(t) &= \tfrac{1}{2}(\omega_1+\omega_2)b_1^2\left({}_a^C D_t^\alpha \phi_1(t)\right)^2+\tfrac{1}{2}\omega_2 b_2^2\left({}_a^C D_t^\alpha \phi_2(t)\right)^2+ \\ &+\omega_2 b_1 b_2 \cos(\phi_1(t)-\phi_2(t))\left({}_a^C D_t^\alpha \phi_1(t)\right)\left({}_a^C D_t^\alpha \phi_2(t)\right)- \\ &-(\omega_1+\omega_2) g b_1 \cos\phi_1(t)-\omega_2 g b_2 \cos\phi_2(t). \end{aligned} \tag{25}$$

The equations of motion for the fractional Hamiltonian are:

Equations (26) describe the motion of a double pendulum system within the Fractional Euler-Lagrange Equations (FELEs) framework, incorporating fractional derivatives to capture memory effects and dynamic coupling. It is presented as:

$$\begin{cases} -\omega_2 b_1 b_2 \sin(\phi_1(t)-\phi_2(t)) \left({}_a^C D_t^\alpha \phi_1(t)\right) \left({}_a^C D_t^\alpha \phi_2(t)\right) + (\omega_1+\omega_2) g b_1 \sin\phi_1(t) = \\ = (\omega_1+\omega_2) b_1^2 {}_t^C D_b^\alpha \left({}_a^C D_t^\alpha \phi_1(t)\right) + \omega_2 b_1 b_2 {}_t^C D_b^\alpha \left(\cos(\phi_1(t)-\phi_2(t)) \left({}_a^C D_t^\alpha \phi_2(t)\right)\right) \\ \omega_2 b_1 b_2 \sin(\phi_1(t)-\phi_2(t)) \left({}_a^C D_t^\alpha \phi_1(t)\right) \left({}_a^C D_t^\alpha \phi_2(t)\right) + \omega_2 g b_2 \sin\phi_2(t) = \\ = \omega_2 b_2^2 {}_t^C D_b^\alpha \left({}_a^C D_t^\alpha \phi_2(t)\right) + \omega_2 b_1 b_2 {}_t^C D_b^\alpha \left(\cos(\phi_1(t)-\phi_2(t)) {}_a^C D_t^\alpha \phi_1(t)\right). \end{cases} \tag{26}$$

These equations generalize classical equations of motion by incorporating fractional derivatives, enabling the study of systems with hereditary or memory-dependent effects.

The figure illustrates the dynamic evolution of a system governed by the FELE for a fractional order of $\alpha = 0.5$.
It illustrates the chaotic and complex dynamics inherent in the fractional double pendulum system.

- Case 1: $\phi_1 = 0.1, \dot{\phi}_1 = 0, \phi_2 = 0.1, \dot{\phi} = 0$
- Case 2: $\phi_1 = 0.1, \dot{\phi}_1 = 0, \phi_2 = 0.8, \dot{\phi} = 0$
- Case 3: $\phi_1 = 0.1, \dot{\phi}_1 = 0, \phi_2 = 1.5, \dot{\phi} = 0$
- Case 4: $\phi_1 = 0.1, \dot{\phi}_1 = 0, \phi_2 = 3.1, \dot{\phi} = 0$
- Case 5: $\phi_1 = 1.5, \dot{\phi}_1 = 0, \phi_2 = 3.1, \dot{\phi} = 0$

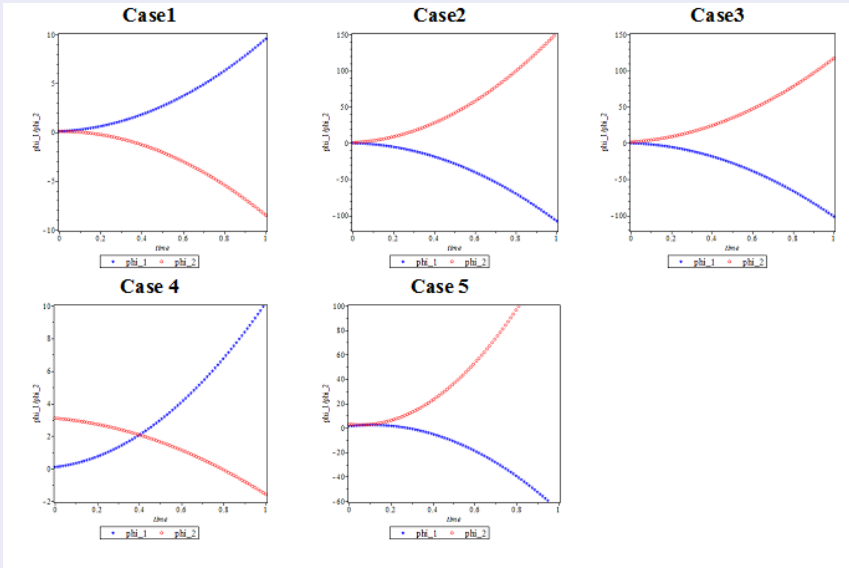

Figure 2: The behavior of the solution for $\alpha = 0.5$ in the FELE equations

2.2. Numerical Study of the Motion of a heavy bead sliding on a rotating wire

J Asad, O Florea, H Khalilia Bulletin of the Transilvania University of Brasov. Series III: Mathematics and Computer Science, 2020

Consider a heavy ball slipping on a rotating wire, with angular frequency ω. The wire deviated away from the vertical axis by an angle ψ .

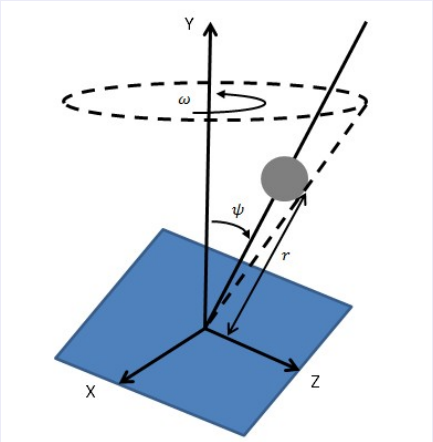

Figure 3: Heavy ball sliding on a rotating wire: This system is used to model the interplay between gravitational, centrifugal, and inertial forces on a constrained mass, revealing complex dynamics under varying initial conditions.

The kinetic energy and the potential energy of the ball:

$$T = \frac{1}{2} m \left(\dot{r}^2 + r^2 \omega^2 \sin^2 \psi \right) \tag{27}$$

This equation captures the translational and rotational contributions to the kinetic energy.

$$V = mgr \cos \psi \tag{28}$$

This reflects the influence of gravity on the system based on the radial position and tilt angle.

The classical Euler-Lagrange equation (CELE) $\frac{\partial L}{\partial r} - \frac{d}{dt} \frac{\partial L}{\partial \dot{r}} = 0$

$$\ddot{r} = r\omega^2 \sin^2 \psi - g \cos \psi \tag{29}$$

This equation describes the motion of the ball in terms of the radial acceleration $\ddot{r}$ and the forces acting on it, including centrifugal and gravitational forces.

The Hamilton system will be:

$$\begin{cases} \dot{r} = \dfrac{\partial H}{\partial p} \\ \dot{p} = -\dfrac{\partial H}{\partial r} = mr\omega^2 \sin^2\psi - mg\cos\psi \end{cases} \tag{30}$$

H= Hamiltonian function representing the total energy of the system.
p= Momentum conjugate to r.

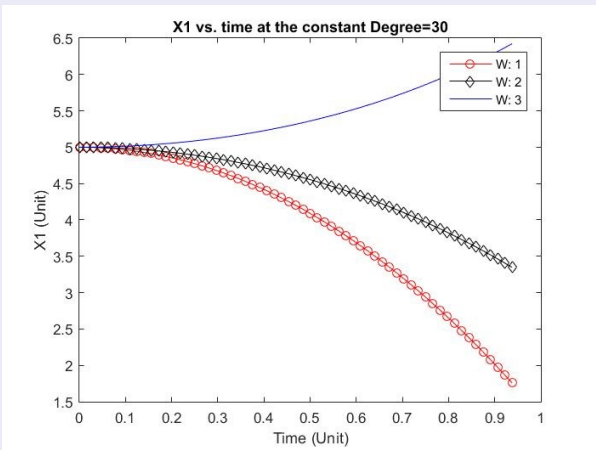

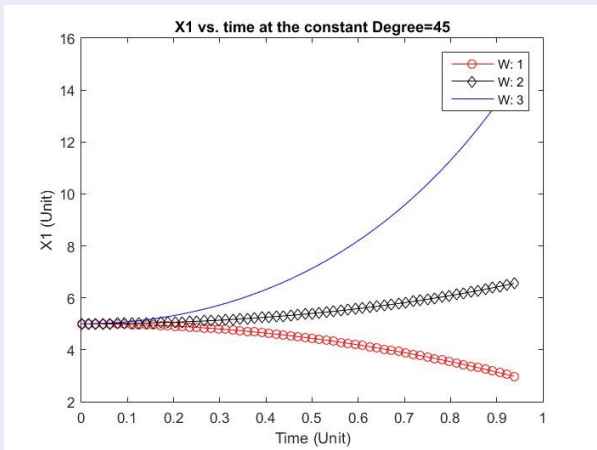

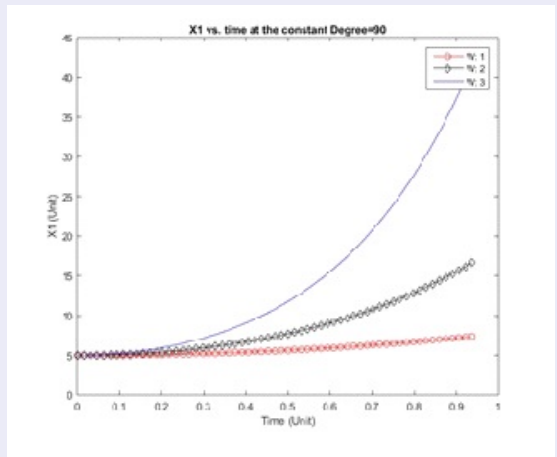

Figure 4: a graphical representation of the behavior of the radial distance r over time for a heavy ball sliding on a rotating wire. The graphs consider varying conditions for the tilt angle $\psi = \{\frac{\pi}{6}, \frac{\pi}{4}, \frac{\pi}{2}\}$ and angular velocity $\omega = \{1, 2, 3\}$.

2.3. Mathematical and numerical approach for telegrapher equation

H SHANAK, O FLOREA, N ALSHAIKH, A Jihad ACTA TECHNICA NAPOCENSIS-Series: APPLIED MATHEMATICS, MECHANICS, and ENGINEERING, 2020

Transmission line represents a long electrical conductor with resistance R, inductance L, capacitance C, and conductance G.

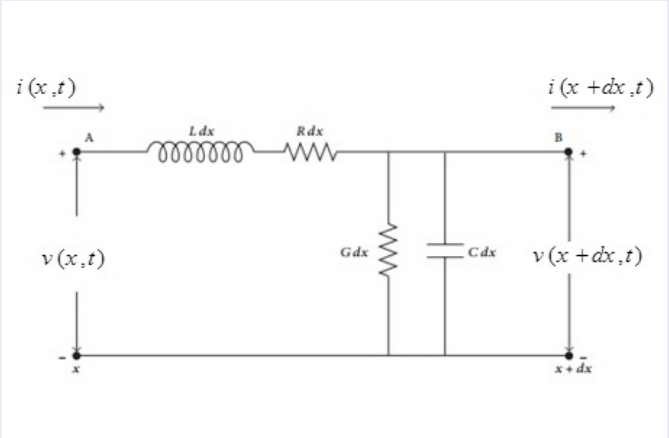

Figure 5: a schematic representation of an electrical transmission line described by the telegraph equation. The model incorporates the physical elements of the line and their effects on voltage $v(x, t)$ and current $i(x, t)$ over time and distance.

Telegraph Equation (With Losses)

$$c^2 \frac{\partial^2 i}{\partial x^2} = \frac{\partial^2 i}{\partial t^2} + (n+m)\frac{\partial i}{\partial t} + (nm)i. \tag{31}$$

$x =$ the distance from sending end of the cable;
$v(x,t) =$ the voltage at any point and any time, on the cable;
$i(x+dx,t) =$ the current at any point and any time, on the cable;
$R =$ the resistance of the cable; $C =$ the capacitance to the ground;
$L =$ the inductance of the cable; $G =$ the conductance to the ground.
$n = \frac{G}{C}$, $m = \frac{R}{L}$, and $c^2 = \frac{1}{LC}$
This equation models the current's time and spatial evolution, considering losses from resistance R and conductance G.

Ideal Lossless Telegraph Equation

For an ideal lossless transmission line $R = 0$ and $G = 0$ the transmission is governed solely by the inductance L and capacitance C per unit length, resulting in ideal wave propagation without attenuation.

$$c^2 \frac{\partial^2 i}{\partial x^2} = \frac{\partial^2 i}{\partial t^2}. \tag{32}$$

The evolution in time of the intensity of the current that passes through the transmission line of the telegrapher

We realized a parallel using the numerical analysis between equation (31) and equation (32).

$i(x,0) = \sin x,\ \frac{\partial i(x,0)}{\partial t} = -\sin x, i(0,t) = 0,$ and $i(1,t) = 0$

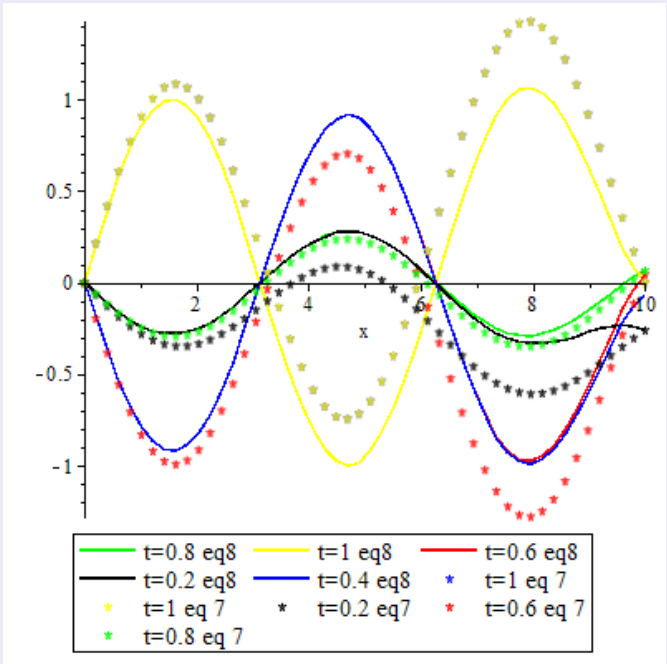

Figure 6: The comparison highlights how losses (represented by R and G) attenuate the signal in equation (31) compared to the ideal case of equation (32).

2.4. Numerical aspects of two coupled harmonic oscillators

Jihad Asad, Olivia Florea in The Scientific Annals of Ovidius University of Constanța. Mathematics Series, 28(1): 5-15, 2020

A two coupled harmonic oscillators of three masses connected linearly by two springs each of stiffness k.

The setup reflects a molecular system where the central mass M represents the atom in the middle of a molecule, and the end masses m mimic the outer atoms. The system can exhibit oscillatory behavior depending on the initial conditions and the spring stiffness.

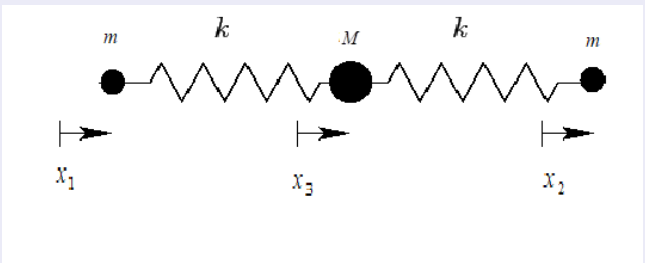

Figure 7: a system of three masses connected by two springs, representing a symmetric linear triatomic molecule CO_2.

The classical Lagrangian $L = T - V$:

$$L = \frac{1}{2}\omega_1 \dot{x}_1^2 + \frac{1}{2}\omega_2 \dot{x}_2^2 + \frac{1}{2}\omega_3 \dot{x}_3^2 - \frac{1}{2}k(x_3 - x_1)^2 - \frac{1}{2}k(x_2 - x_3)^2 \tag{33}$$

This Lagrangian describes the interaction of the masses through the springs and their motions.

The classical Euler- Lagrange Equations (CELE's)

$$r\ddot{x}_1 = -\Omega^2((1+r)x_1 + x_2) \tag{34}$$

$$r\ddot{x}_2 = -\Omega^2((1+r)x_2 + x_1) \tag{35}$$

where $r = \frac{M}{m}$, and $\Omega = \sqrt{\frac{k}{m}}$.
These equations illustrate the coupled motion of the system, highlighting the dependency of the second mass's motion on the first and vice versa.

Symmetric (Breathing) Mode of Oscillation

- Figure 8 illustrates the symmetric mode of oscillation for the system of two coupled harmonic oscillators with three masses (two identical end masses m and a central mass M).
  The system exhibits oscillations where the displacement of the end masses is symmetric, creating a "breathing" effect.
  The central mass remains at rest, acting as a node of oscillatory motion.

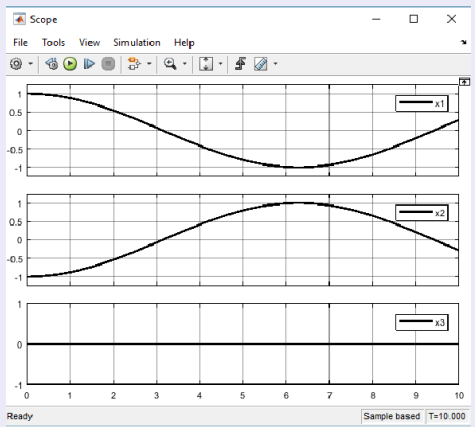

Figure 8: The behavior of the solutions of the system in the case when r=1.5 and $\Omega = \sqrt{\frac{k}{m}} = 0.50$

Asymmetric Mode of Oscillation

- Figure 9 depicts the asymmetric mode of oscillation, where the dynamics differ from the symmetric mode.
  This mode highlights the relative motion of the central mass against the synchronized movement of the end masses.
  The central mass's displacement is scaled inversely by the mass ratio.

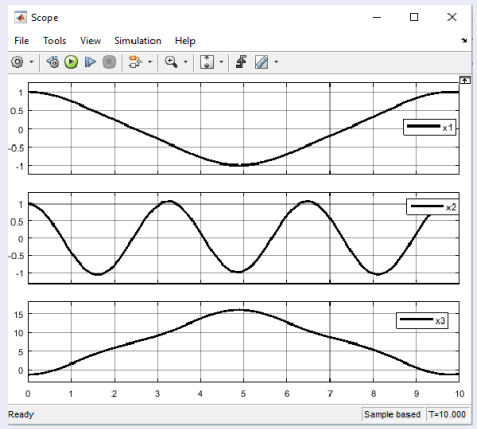

Figure 9: The behavior of the solutions of the system in the case when r=1.5 and $\Omega = \sqrt{\frac{k}{m}} = 0.50$

Chapter 3. Innovative Modeling Approaches in Nanomaterials and Biomass Analysis

- The thesis applies insights from nonlinear dynamics to practical problems in nanomaterials and biomass combustion.
- In nanotechnology, it models the chaotic behavior of Barium Titanate nanoparticles using a photonic tunneling framework, which is significant for developing materials in electronics and multiferroic devices.
- For biomass and sustainable energy, the research investigates the porosity of wood briquettes, highlighting how porosity impacts combustion efficiency. This work offers potential improvements in biomass fuel technology, supporting cleaner and more efficient energy production.

3.1. Microscopic Hamiltonian and chaotic behavior for Barium Titanate nanoparticles revealed by photonic tunneling model

E Godwe, O Florea, R Jarrar, M Justin, J Asad Physics Letters A, 2023

- Photon field couplings are formed between many-body electrons. In our study we will focus on photons whose finite mass is made up of interacting electrons.
- based on Ehrenfest's theorem, we will use the method of derivation of semi-quantal dynamics due to the fact that its approach is closer to the formulations of non-equilibrium static mechanics.

The explicit form of the dynamics equation from the photonic tunneling model in ferroelectrics

Dynamics of Photon Position and Momentum

$$\frac{dx}{dt} = \frac{p}{mN},; \qquad \frac{dp}{dt} = 2k^2x_0^2x - 2k^2x^3 - 6k^2x\,\rho^2 \tag{36}$$

Dynamics of Auxiliary Parameters

$$\frac{d\rho}{dt} = \xi; \qquad \frac{d\xi}{dt} = \frac{1}{4\rho^3} + \rho\left(2k^2x_0^2 - 6k^2x^2\right) - 6k^2\rho^3. \tag{37}$$

$p =$ the photon's momentum; $x =$ the photon's position.
$m =$ the mass of the electron -photon is , $N =$ the average number of electro-photons in a finite standard block spin
$\omega =$ the tunneling frequency for a double well potential appropriate to the KDP-type crystals.
$\rho =$ Auxiliary parameter related to photonic energy distribution.
$\xi =$ additional parameter capturing the temporal evolution of ρ.

The effective Hamiltonian associated to Barium Titanate ferroelectric

The Hamiltonian H_{ext} provides a comprehensive description of the total energy of the system, integrating kinetic, potential, and auxiliary energy terms.

$$H_{ext} = \frac{P^2}{2} + \frac{\xi^2}{2} + V_{ext}(x, \rho), \tag{38}$$

The potential V_{ext} incorporates nonlinear effects, such as quartic terms (x^4, ρ^4)) and coupling between position (x) and auxiliary variables ρ.

$$\begin{aligned} V_{ext}(x, \rho) = & \frac{1}{2}k^2\left(x^4 - 2x_0^2x^2 + x_0^4\right) + \frac{1}{8\rho^2} \\ & + k^2\rho^2\left(3x^2 - x_0^2\right) + \frac{3}{4}k^2\rho^4 \end{aligned} \tag{39}$$

These equations are central to studying photonic tunneling in ferroelectric materials, with applications in nonlinear optics and electronic devices.

Figure[10] displays the Poincaré sections for a system governed by photonic tunneling dynamics in ferroelectrics under a double-well potential. The figure illustrates the chaotic and stable regimes based on the parameter k, the coupling constant.

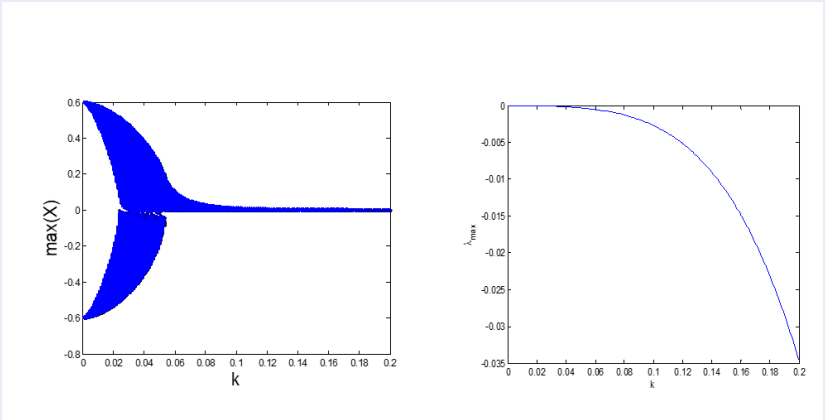

Figure 10: Poincare sections in the plane (ξ, x). We set parameters as $k = 0.22$; $x_0 = 10$; $m = 0.00278$; with the initial conditions (0.3; 0.3; 0.01; 0.01).

For $k < 0.05$ the system contains no stable fix point and then becomes chaotic.
For $k > 0.05$ the trajectory converges towards the equilibrium point.

- the Lyapunov exponent estimated is positive when the parameter k is below 0.05, a positive exponent implies the divergence of neighboring trajectories, i.e. for these values of the system parameters, and we have a chaotic behavior.
- the Lyapunov exponent is negative when the parameter k is over 0.05 that is to say the system is stable in this domain.

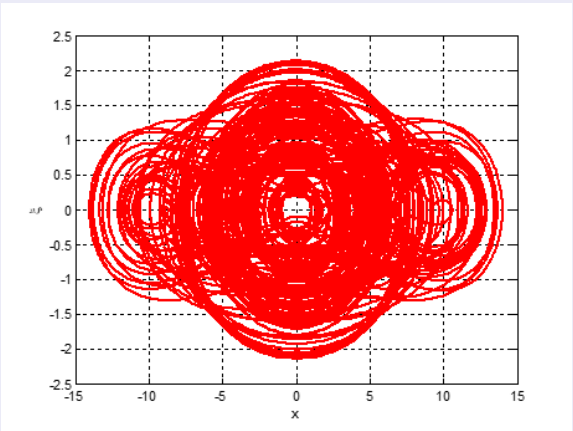

Figure 11: Dynamics with respect to the bifurcation diagram for $x_0 = 10$ under the effect of the tunneling frequency ω and the maximal Lyapunov exponent for the set of equations (36) versus the parameter k with the initial conditions (0.3; 0.6; 0.1; 0.1).

3.2. Indirect evaluation of the porosity of waste wood briquettes by assessing their surface quality

D Sova, L Gurau, M Porojan, O Florea, V Sandu, M Purcaru Waste and Biomass Valorization, 1 -15, 2022

- Briquettes are porous materials. During immersion, a part of the pores (voids developed during chips compression) is filled with liquid.
- pelletizing and briquetting are the most common processes used for biomass densification for solid fuel applications.

the briquettes' porosity was calculated by using three methods

- Hunt determined the oven-dry wood cell porosity (P_d) from the oven-dry density (ρ_{OD}), the density of the cell wall (ρ_{cw}) and the density of air (ρ_{air}), by using the following equations:

$$\rho_{\mathrm{OD}} = \rho_{cw}(1 - P_d) + \rho_{air}P_d \tag{40}$$

and

$$P_d = \frac{\rho_{cw} - \rho_{\mathrm{OD}}}{\rho_{cw} - \rho_{air}} \tag{41}$$

The density can be expressed as:

$$\rho = \rho_{cw_M}(1 - P) + \rho_{air}P \tag{42}$$

where: $\rho_{cw_M}$is the density of the cell wall with bound water. The wet porosity is obtained from Eq. (42), as follows:

$$P = \frac{\rho_{cw_M} - \rho}{\rho_{cw_M} - \rho_{air}} \tag{43}$$

- A second method, calculating the wood porosity in wet conditions, based on Siau's equation is:

$$P = 1 - \frac{\omega_{\mathrm{OD}}}{1000\ V_{br.}}(0.653 + 0.01M) \tag{44}$$

where: P is the porosity or the fractional void volume of wood, 0.653×10^{-3} (m^3/kg) is the specific volume of the wood substance, M (%) is wood moisture content.

- The third method used for wood porosity calculation, which was proposed by Hunt et al. is based on dry cell porosity and moisture content.
  Wet porosity is:

$$P = \frac{(1 - V\%_{bw})\, P_d}{1 - V\%_{bw} P_d} \tag{45}$$

where: $V\%_{bw}$ is the bound water volume fraction.

Chapter 4. Further research

4.1. A qualitative analysis on the double porous thermoelastic bodies with microtemperature

Florea, OA ; Craciun, EM; Öchsner, A; Emin, AN, CONTINUUM MECHANICS AND THERMODYNAMICS, Volume36, Nov 2024

The thermal displacement m depends on the temperature variation θ, between two states of the body

$$m(x,\xi) = \int_{\xi_0}^{\xi} \theta(x,s)ds, \tag{46}$$

This equation represents the cumulative effect of temperature changes over time on thermal displacement.

The microthermal displacement ν_i depends on the variation of microtemperatures $\mathcal{T}_i$ between two states of the body:

$$\nu_i(x,\xi) = \int_{\xi_0}^{\xi} \mathcal{T}_i(x,s)ds, \tag{47}$$

where $\mathcal{T}_i(x,\xi) = \Theta_i(x,\xi) - T_{0i}$. Microthermal displacement ν_i is influenced by and influences mechanical displacement fields, creating a feedback loop between thermal and elastic properties.

The energy equations for thermoelastic materials with double porosity and microtemperature effects are formulated as follows:

$$\begin{aligned} \rho\dot{\eta} &= Q_{j,j} + \rho\mathfrak{h}, \\ \rho\dot{\eta}_i &= Q_{ji,j} + \rho\mathfrak{h}_i. \end{aligned} \tag{48}$$

- ρ: Density of the material, η: Entropy of the system,
- η_i: Microtemperature-related entropy terms,
- Q_j: Heat flux components, Q_{ji}: Microtemperature heat flux components,
- h: Heat supply to the system, h_i: Microtemperature heat supply.

These equations are essential for modeling energy transfer and thermal dissipation in advanced materials, particularly those with complex microstructural properties.

We will consider the following hypotheses:
(a) the coefficients from the equations that govern the thermoelastic body are positive: $\rho > 0$, $K_1 > 0$, $K_2 > 0$ și $\omega > 0$,
(b) the free energy is a positively semi-definite function,
(c) the conductivity coefficients D_{ij} are the components of a tensor defined so that $\exists\, d_0 > 0$: $D_{ij}\zeta_i\zeta_j \geq d_0\zeta_i\zeta_i$, for all ζ_i.

The initial conditions for the mixed problem of thermoelastic bodies with double porosity and microtemperature are:

$$\begin{aligned} u_i(x,0) &= u_{i0}(x), \quad \dot{u}_i(x,0) = u_{i1}(x), \\ \varphi(x,0) &= \varphi_0(x), \quad \dot{\varphi}(x,0) = \varphi_1(x), \\ \psi(x,0) &= \psi_0(x), \quad \dot{\psi}(x,0) = \psi_1(x), \\ m(x,0) &= m_0(x), \quad \dot{m}(x,0) = m_1(x), \\ \nu_i(x,0) &= \nu_{i0}(x), \quad \dot{\nu}_i(x,0) = \nu_{i1}(x), \end{aligned} \tag{49}$$

These initial conditions ensure the problem is well-posed, defining a clear starting point for solving the equations of motion, volume fraction evolution, and thermal effects. They are critical for guaranteeing uniqueness and stability of the solution.

the boundary conditions:

$$\begin{aligned} u_i(x,\xi) &= u_i^b(x,\xi), \\ \varphi(x,\xi) &= \varphi^b(x,\xi), \\ \psi(x,\xi) &= \psi^b(x,\xi), \\ m(x,\xi) &= m^b(x,\xi), \\ \nu_i(x,\xi) &= \nu_i^b(x,\xi), \end{aligned} \tag{50}$$

These boundary conditions ensure that the behavior of the system at its edges or interfaces conforms to external constraints or applied conditions, such as:
Fixed displacements or movements at the boundaries.
Specified thermal or microthermal effects.
Controlled volume fractions for porous structures.

Lemma

The influence of the microtemperatures on a double porous thermoelastic body leads to obtaining a thermic deformation, expressed by the following equation:

$$\begin{aligned} u_{i,j}t_{ij} + \varphi_{,i}\sigma_i + \psi_{,i}\tau_i + \varphi\mathfrak{p} + \psi\mathfrak{r} + m_{,i}Q_i + \nu_{i,j}Q_{ij} + \rho(\eta\dot{m} + \eta_i\dot{\nu}_i) = \\ = M_{ijkl}u_{i,j}u_{k,l} + B_{ij}\varphi_{,i}\varphi_{,j} + C_{ij}\psi_{,i}\psi_{,j} + a_1\varphi^2 + a_2\psi^2 \\ + d_{ij}m_{,i}m_{,j} + e_{ijkl}\nu_{i,j}\nu_{k,l} + \omega\dot{m}^2 + E_{ij}\dot{\nu}_i\dot{\nu}_j \\ + 2(N_{ij}u_{i,j}\varphi + P_{ij}u_{i,j}\psi + a_{ijkl}u_{i,j}\nu_{k,l} + A_{ij}\varphi_{,i}\psi_{,j} \\ + b_{ij}\varphi_{,i}m_{,j} + c_{ij}\psi_{,i}m_{,j} + R_{ij}\varphi\nu_{i,j} + a_3\varphi\psi + S_{ij}\psi\nu_{i,j}). \end{aligned} \tag{51}$$

The lemma emphasizes the interplay between thermal gradients, microtemperatures, and mechanical displacements, establishing a rigorous mathematical foundation for the energy interactions within the system.

Theorem

Let us consider a thermoelastic body with double porosity under the action of microtemperatures in which the symmetry equations are fullfiled. If the hypotheses $(a) - (c)$ *are simultaneos satisfied, then the mixed problem with the initial conditions* (49) *and the boundary conditions* (50) *admits at most one solution.*

This theorem guarantees:
Predictability: The system's behavior is uniquely determined by the given conditions.
Stability: Ensures the model's reliability for engineering applications.
Physical Consistency: Confirms that the model aligns with real-world observations, making it a robust framework for studying thermoelastic materials.

the study of the existence of the solution of the mixed problem

We will consider an evolution equation defined in a suitable chosen Hilbert space $\mathcal{H}$. The Hilbert space provides a mathematical framework to rigorously define the function spaces where the solutions exist.

$$\mathcal{H} = \left[\mathbf{W}_0^{1,2} \times \mathbf{L}^2\right]^5, \tag{52}$$

The Sobolev space $\mathbf{W}_0^{1,2}$ accommodates the displacement fields, which need to have finite strain energy (derivatives are square-integrable).
The $\mathbf{L}^2$ space supports fields like microtemperature variations, ensuring they are physically measurable (finite energy).

Theorem

We will consider the vector functions:

$$\begin{aligned} \mathrm{U} &= (u_i, v_i, \varphi, \Phi, \psi, \Psi, m, \Lambda, \nu_i, V_i)\,, \\ \mathrm{U}' &= (u_i', v_i', \varphi', \Phi', \psi', \Psi', m', \Lambda', \nu_i', V_i')\,. \end{aligned} \tag{53}$$

The norm of the scalar product $\langle \mathrm{U}, \mathrm{U}' \rangle = J_1 + J_2$, *where*

$$\begin{aligned} J_1 &= \tfrac{1}{2} \int\limits_B (\rho v_i v_i' + K_1 \Phi \Phi' + K_2 \Psi \Psi' + \omega \Lambda \Lambda' + E_{ij} V_i V_i')\ dV, \\ J_2 &= \tfrac{1}{2} \int\limits_B F(\mathrm{U}, \mathrm{U}')\ dV, \end{aligned} \tag{54}$$

J_1 *represents inputs from kinetic and thermal energy.*
J_2 *represents additional interaction terms.*
This equivalence is crucial for proving the stability and robustness of solutions within the Hilbert space framework.

Pendulum between Two springs using Ms- DTM

Olivia A. Florea, Doaa Shahroor, Rania Wannan and Jihad Asad
Physica Scripta - under review

a pendulum system suspended between two horizontal springs

Multi-Step Differential Transformation Method (Ms-DTM) is used to solve the nonlinear equations of motion derived from the system's Lagrangian. The study highlights the superiority of Ms-DTM in handling the complex nonlinearities and stiff equations associated with the system, which are challenging for conventional methods like the Runge-Kutta technique.

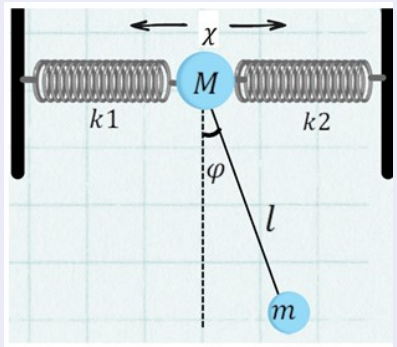

Figure 12: This figure illustrates a mechanical system consisting of a simple pendulum suspended between two horizontal springs. The system is designed to study the interplay between rotational and translational motion, influenced by the elasticity of the springs and the gravitational force.

The kinetic energy ($\mathcal{T}$) of m and $\mathcal{M}$ can easily be shown that:

$$\mathcal{T} = \frac{1}{2}\mathcal{M}\dot{\chi}^2 + \frac{1}{2}m\dot{\chi}^2 + \frac{1}{2}m\ell^2\dot{\phi}^2 + m\ell\dot{\phi}\dot{\chi}cos\phi. \tag{55}$$

the potential energy ($\mathcal{V}$): the gravitational potential energy ($\mathcal{V}_g$), and the potential energy due to the two springs ($\mathcal{V}_s$).

$$\mathcal{V} = \mathcal{V}_g + \mathcal{V}_s = -mg\ell cos\phi + \frac{1}{2}\kappa_1\chi^2 + \frac{1}{2}\kappa_2\chi^2. \tag{56}$$

This equation represents the total kinetic energy, accounting for both translational χ and rotational ϕ movements.

The Euler-Lagrange Equations (ELEs) derived from the dynamics of a pendulum suspended between two springs are:

$$\ddot{\chi} + \left(\frac{m\ell}{m+\mathcal{M}}\right)\ddot{\phi} - \left(\frac{m\ell}{m+\mathcal{M}}\right)\dot{\phi}^2\phi + \left(\frac{\kappa_1+\kappa_2}{m+\mathcal{M}}\right)\chi = 0. \tag{57}$$

$$\ddot{\phi} + \frac{1}{\ell}\ddot{\chi} + \omega_o^2\phi = 0. \tag{58}$$

Multi-Step Differential Transform Method (MS-DTM)

$$\begin{cases} (k+1)(k+2)\Phi(k+2)+\frac{1}{l}(k+1)(k+2)\mathbb{X}(k+2)+\omega_0\Phi(k) = 0 \\ (k+1)(k+2)\mathbb{X}(k+2)+a(k+1)(k+2)\Phi(k+2)+b\mathbb{X}(k)- \\ \qquad -\sum_{l=0}^{k}\sum_{s=0}^{k-l}(s+1)(m+1)\Phi(s+1)\Phi(m+1)\Phi(k-s-m) = 0 \end{cases}. \tag{59}$$

Where $\Phi(k)$ is the differential transformation of the original function $\phi(t)$ and $\mathbb{X}(k)$ is the differential transformation of the original function $\chi(t)$.

The application of MS-DTM allows us to express the general solution of the system (59) as follows:

$$\chi(t)=\begin{cases}\sum_{k=0}^{N}\mathbb{X}_1(k)(t)^k,\ t\in[0,t_1]\\ \sum_{k=0}^{N}\mathbb{X}_2(k)(t-t_1)^k,\ t\in[t_1,t_2]\\ \sum_{k=0}^{N}\mathbb{X}_3(k)(t-t_2)^k,\ t\in[t_2,t_3]\\ \ldots\ldots\ldots\ldots\ldots\ldots\ldots\ldots\ldots\ldots\ldots\ldots\\ \sum_{k=0}^{N}\mathbb{X}_{M-1}(k)(t-t_{M-2})^k,\ t\in[t_{M-2},t_{M-1}]\\ \sum_{k=0}^{N}\mathbb{X}_M(k)(t-t_{M-1})^k,\ t\in[t_{M-1},t_M]\end{cases}. \tag{60}$$

$$\phi(t) = \begin{cases} \sum_{k=0}^{N} \Phi_1(k)(t)^k, t\in[0,t_1] \\ \sum_{k=0}^{N} \Phi_2(k)(t-t_1)^k, t\in[t_1, t_2] \\ \sum_{k=0}^{N} \Phi_3(k)(t-t_2)^k, t\in[t_2, t_3] \\ \dots\dots\dots\dots\dots\dots\dots\dots\dots\dots\dots\dots \\ \sum_{k=0}^{N} \Phi_{M-1}(k)(t-t_{M-2})^k, t\in[t_{M-2}, t_{M-1}] \\ \sum_{k=0}^{N} \Phi_M(k)(t-t_{M-1})^k, t\in[t_{M-1}, t_M] \end{cases} . \tag{61}$$

we consider the following parameters κ_1=1;
$\kappa_2 = 1; \ell = 1;\ m = 0.1;\ M = 1.$

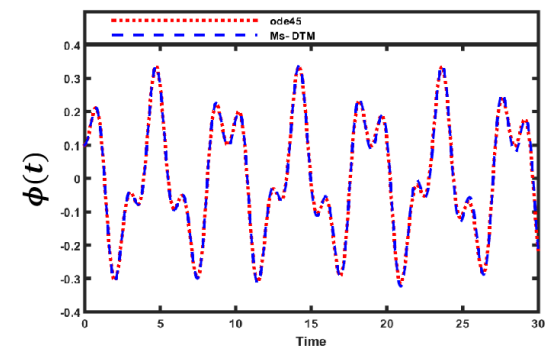

Figure 13: Time evolution of the function ϕ using the Ms-DTM and Runge-Kutta methods.

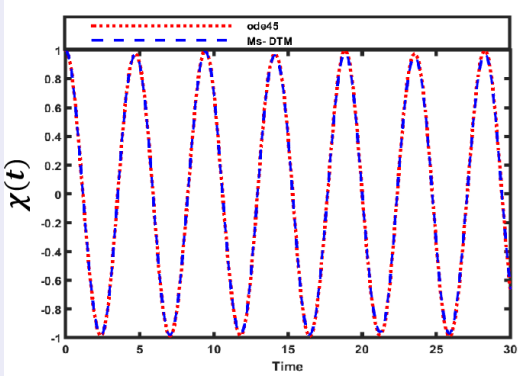

Figure 14: Time evolution of the function χ using the Ms-DTM and Runge-Kutta methods.

Conclusions

- I will continue advancing research in Continuum Mechanics and Dynamical Systems.
- I will continue mentoring students to achieve excellence in these fields.
- I will actively participate in scientific projects that contribute to the advancement of knowledge and technology.
- I am committed to building a strong, vibrant research community.
- I aim to make meaningful contributions to the field of Mathematics and its applications.

Thank you for your attention!